

Study of diffuse instability and controllability in constant shear tests

Mauricio Pinheiro

Thurber Engineering Ltd., Calgary Alberta, Canada

Richard G. Wan

Dept. of Civil Engineering, University of Calgary, Calgary, Alberta, Canada



ABSTRACT

Constant shear tests follow an effective stress path at constant deviator stress with a reduction in mean effective stress. These tests were idealized as a means to simulate soil behaviour during water infiltration processes in slopes leading to failure. Interestingly, laboratory specimens subjected to constant shear paths failed at stress levels far from Mohr-Coulomb failure surface. Although a so-called collapse surface has been previously introduced in the literature to explain this intriguing phenomenon, a more mechanistic approach is to advocate concepts such as Hill's stability and Nova's controllability. In this paper, we numerically analyze some constant shear tests based on the above concepts using a non-associated elastoplastic constitutive model. The analyses range from a Gauss point level to a boundary value problem setting where a three-dimensional cylindrical specimen is simulated.

RÉSUMÉ

Des essais à q constant suivent un chemin de chargement avec déviateur de contrainte constant et réduction en contrainte moyenne effective. Ces essais essentiellement représentent le comportement d'un point matériel dans une pente menée à la rupture par écoulement d'eau. Il s'avère que lors de ces essais, la rupture le long de ces chemins à q constant est strictement à l'intérieure de la condition de plasticité de Mohr-Coulomb. Toutefois, bien qu'on puisse classiquement introduire une surface d'effondrement (collapse surface) pour expliquer ce phénomène, une approche plus adaptée au point de vue mécanique consisterait en une analyse basée sur la condition de stabilité de Hill ou de contrôlabilité au sens de Nova. Dans cet article, on présente une modélisation numérique des essais à q constant dans le cadre de l'instabilité matérielle ou de la contrôlabilité avec une loi constitutive non-associée. Ces calculs sont menés en un point matériel et ensuite généralisés au cas d'un problème à frontières à travers l'exemple d'un échantillon cylindrique en 3D.

1 INTRODUCTION

A physical interpretation of instability generally evokes the idea that a small perturbation results into an unbounded output. In this respect, the conventional plastic limit failure defined by the Mohr-Coulomb criterion can be viewed as a problem of instability whereby a small or null stress input leads to large deformations. Conversely, experimental, theoretical and numerical findings have demonstrated that a material may also display unstable behaviour even before such limit state is reached (Darve 1994, Lade 2002, Chu et al. 2003). For instance, strain localization has been observed before peak conditions in a drained triaxial test on sand (Desrues & Viggiani 2004). As for undrained tests on loose sand, plastic instability at the peak of deviatoric stress is obtained at a level well below the plastic limit state. Hence, this well-known static liquefaction phenomenon underlies two important aspects of failure, namely diffuse deformations in the absence of strain localization and the notion of controllability (Nova 1994, Imposimato & Nova 2001). The latter sets the control conditions upon which instabilities may occur as a result of the loss of uniqueness of admissible material response.

We mentioned above the ubiquitous case of loose sand in undrained conventional triaxial tests as a means

to illustrate the role played by diffuse instability in the material deformation. Throughout this paper, though, we will focus on another type of stress path and loading conditions that according to Chu et al. (2003) lacks further investigation. We refer to constant shear tests. In these tests the deviator stress is kept constant while the mean effective stress is reduced. Consolidation and conventional triaxial shearing phases normally precede these tests in order to set the specimen to a prescribed stress state. Constant shear tests were earlier idealized to emulate soil response during water infiltration process of slopes led to failure (Brand 1981, Sasitharan et al. 1993). The practical importance of these unloading tests lies on the fact that if they were carried out by imposing fluid flux inside the specimen, diffuse collapse would develop as soon as stress states concomitantly reached the instability zone yet far away from the plastic limit surface. In our numerical simulations, solution breaks down at that point.

This paper is subdivided into three main parts. In the first part, various forms of bifurcations and instabilities in geomaterials are reviewed in order to set the stage for the subsequent computational analysis. Attention will be given to diffuse instability and the notion of controllability. The second part brings forth the numerical computations performed at element level. Here a series of constant

shear tests is numerically simulated in order to explore the role played by the control parameters. Especially important in these numerical analyses is to realize the existence of domains within the plastic limit surface where instability may take place. In the final section, the computations are extended to a boundary value problem setting where diffuse flow failure of a three-dimensional cylindrical specimen is examined. Similar tests as those performed at element level are regarded here again. The soil specimen will be taken as a heterogeneous medium where a spatially non-correlated normal (Gaussian) distribution of void ratio is assumed. Such a perturbation in the specimen homogeneous character is shown to be essential in order to induce diffuse instability.

2 DIFFUSE INSTABILITY AND CONTROLLABILITY

2.1 Diffuse Instability

The notion of diffuse instability is closely link to the stability of deforming solids subject to small disturbance. That is, applying a kinematically admissible velocity field to an equilibrium state under dead loading, the increase in internal energy minus the work of external forces should be positive for stability. Based on this premise, Hill (1958) worked out the so-called second-order work criterion as the product of incremental stress and strain during a loading increment. From an engineering application viewpoint, diffuse instability can be mathematically captured by the violation of Hill's stability criterion defined by the sign of the second-order work. Whenever the second-order work becomes nonpositive at a material point, the material response has become locally unstable. Then, if the loss of positiveness of the second-order work becomes pervasive within the structure, collapse may eventually occur. For a given nonzero strain increment $d\boldsymbol{\epsilon}$ the second-order work criterion is locally expressed as below:

$$W_2 = d\boldsymbol{\sigma} \cdot d\boldsymbol{\epsilon} \quad [1]$$

where we note the incremental constitutive relation given by $d\boldsymbol{\sigma} = \mathbf{D} \cdot d\boldsymbol{\epsilon}$; \mathbf{D} is the constitutive tensor (matrix).

The concept of second-order work, which may underlie a bifurcation problem, can be extended to highlight the link between instability, loading direction and response behaviours of a material. For instance, we have demonstrated that the domain of stress-strain states for which at least one loading-response direction exists such that the second-order work becomes non-positive gives rise to a so-called bifurcation domain (Wan et al. 2009). This concept though, has to be brought hand-in-hand with that of controllability as we will demonstrate in the next section.

In light of above discussion, it can be shown that if at least one zero-valued eigenvalue of the constitutive tensor \mathbf{D} exists, then the associated eigentensor, \mathbf{v} , will lead the material to a bifurcated state. That can be realized by

assigning $d\boldsymbol{\epsilon} = \mathbf{v}$ and recasting the second-order work expression in Eq. [1] into the form below:

$$W_2 = d\boldsymbol{\epsilon}^T \cdot \mathbf{D} \cdot d\boldsymbol{\epsilon} > 0 \quad [2]$$

which is reminiscent of an associated quadratic form wherein the positive definiteness of the constitutive tangent tensor implies that the second-order work is positive.

2.2 Controllability

In a lab experiment, a soil specimen may be subject to different loading programmes whereby either forces or displacements or a mix of both are being controlled simultaneously. It may happen that during the course of loading one or a combination of these control parameters can no longer be controlled. Nova (1994) referred to that phenomenon as loss of controllability, a concept synonym to non-uniqueness of the incremental solution in theoretical continuum mechanics. He also showed that the occurrence of diffuse and localized instabilities can be treated within this framework (Nova 2003).

The mathematical structure involving the notion of controllability has been well explored in Nova (1994, 2003). Thus, we only briefly explain it here.

Let the material incremental response be described by the equation below:

$$\mathbf{C} \cdot d\boldsymbol{\sigma} = d\boldsymbol{\epsilon} \quad [3]$$

where $d\boldsymbol{\epsilon}$ acts as controlled parameters (say, controlled by the machine test operator) and $\mathbf{C} = \mathbf{D}^{-1}$.

More generally though, part of the stress and strain components or a combination of these may be controlled at the same time, such as, e.g. in the conventional triaxial test in soil mechanics, where the specimen's top surface is load in displacement control mode while an all-around confining stress is kept constant throughout the test.

In a general case, Eq. [3] needs to be reorganized as follows:

$$\mathbf{M} \cdot d\mathbf{r} = d\boldsymbol{\theta} \quad [4]$$

where $d\boldsymbol{\theta} \neq \mathbf{0}$ contains the controlled parameters; $d\mathbf{r}$ contains the measured/response variables. \mathbf{M} symbolizes the new constitutive matrix.

Under such general loading programme, control of the test is lost whenever $\det \mathbf{M}$ is zero. Nova (1994) yet shows that whenever a principal minor of the original \mathbf{C} is zero, there exists a loading programme where control is lost and thus non-uniqueness appears. That leads to a corollary: controllability and uniqueness are guaranteed if \mathbf{C} is positive definite; which in turn is closely linked with the positiveness of Hill's second-order work in Eq. [1].

3 CONSTANT SHEAR TESTS

Constant shear tests are those where the deviatoric stress ($q = \sigma_1 - \sigma_3$ in axisymmetric conditions) is kept constant while the mean effective stress is reduced. Consolidation and shearing phases normally precede these tests in order to set the specimen to a desired stress state. Constant shear tests were earlier idealized as a means to simulate the soil behaviour during water infiltration process of slopes led to failure (Brand 1981; Sasitharan et al. 1993). As water infiltration advances, internal pore water pressure increases slowly and mean effective stresses reduce provided that external loads remain unchanged. The deviatoric stress stays constant.

In this section, we present and discuss a few experimental results from constant shear tests reported in the literature. As for illustrative purposes, Figure 1 shows a series of constant shear tests on Hostun S28 sand under axisymmetric conditions reported in Darve et al. (2007). Both drained (CSD) and undrained (CSU) conditions were explored at various stress levels. Curiously, all specimens showed unstable response and loss of test controllability roughly by a single line in the p - q plot. Unstable response of the test was marked by the inability of the operator to control the test according to the loading program. For instance, referring to test CSD#1 in Figure 1, maintenance of a constant q under drained conditions could not be satisfied anymore at some point during loading history when the sample suddenly succumbed to escalating axial strains. The deformation pattern involved a collapsing structure with no visible localization pattern within the kinematic field (Darve et al. 2007). Also, this loss of controllability depends apparently on the loading program, i.e. loading direction. As a generalization of the latter, the locus of points for which instability occurs for a given loading direction defines a boundary in the p - q plot whose existence can be explained within Hill's second-order work framework.

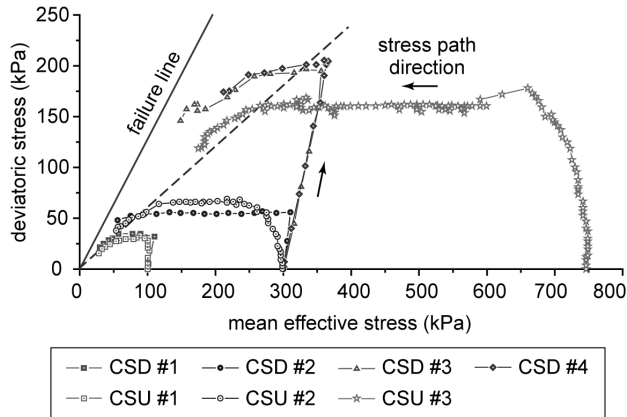


Figure 1. Drained constant shear tests and undrained constant shear tests performed on Hostun S28 sand at various stress levels (data from Darve et al. 2007).

4 STABILITY ANALYSIS

The prototype tests we analyze in this section refer to axisymmetric stress-strain conditions. They are carried out in three steps: (a) soil specimen is isotropically consolidated to a given stress level ($d\sigma_1 = d\sigma_3 > 0$, where 1 = axial direction, 3 = radial direction); (b) shear loading continues along a triaxial compression path under drained condition up to a prescribed deviatoric stress level ($d\sigma_1 > 0$, $d\sigma_3 = 0$); (c) the mean effective stress is either directly or indirectly decreased while the deviatoric stress is being kept constant ($d\sigma_1 = d\sigma_3 < 0$). From a numerical standpoint, a direct method of simulating the tests consists in decreasing the effective stress components under drained conditions. However, in lab testing, there are two ways to indirectly decrease the mean effective stress, namely, by either increasing the pore water pressure at constant total stress or forcing the sample to dilate ($d\varepsilon_v < 0$) by water injection. In our simulations, we have applied both the direct and the forced dilation (injection) methods.

The WG-model will be used to describe the soil behaviour in all numerical simulations. This constitutive model is based on the principles of continuum mechanics and the theory of plasticity but also presents embedded micromechanical information. It is an outgrowth of a double yield surface law initially developed by Wan & Guo (1998) and founded on Rowe's stress-dilatancy theory (Rowe 1962) and the critical state concept (Schofield & Wroth 1968). These two frameworks were combined in order to account for density, stress level, and anisotropy dependencies (Wan & Guo 2001a, b, 2004). More details about this model can be found in the cited references or alternatively in Wan et al. (2008).

4.1 Element test level

The initial mean stress in all tests at element level is 300 kPa. Three distinct levels of deviatoric stresses are investigated, i.e. 50, 100 and 200 kPa. The material studied is a loose sand with an initial void ratio equal to 0.80. Figure 2 shows the simulations of these numerical experiments using the WG-model. The results for the constant shear tests under stress-controlled mode (direct method) are presented in Figure 2a. In Figure 2b, we display similar plots for the very same constant shear tests simulated under mixed-controlled mode (forced dilation).

In axisymmetric stress-strain conditions, the second-order work in Eq. [1] can be defined in terms of the stress and strain invariants as shown below:

$$W_2 = dpd\varepsilon_v + dqd\gamma = \begin{Bmatrix} d\gamma \\ d\varepsilon \end{Bmatrix}^T \begin{bmatrix} D_{11} & D_{12} \\ D_{21} & D_{22} \end{bmatrix} \begin{Bmatrix} d\gamma \\ d\varepsilon \end{Bmatrix} \quad [5]$$

$$\text{with } \begin{Bmatrix} dq \\ dp \end{Bmatrix} = \begin{bmatrix} D_{11} & D_{12} \\ D_{21} & D_{22} \end{bmatrix} \begin{Bmatrix} d\gamma \\ d\varepsilon \end{Bmatrix}$$

where we have expressed the controlling parameters (dp , dq) in terms of the response variables ($d\gamma$, $d\varepsilon_v$) and defined the matrix \mathbf{D} that relates (dp , dq) to ($d\gamma$, $d\varepsilon_v$).

Throughout the constant shear test $dq = 0$ and $dp < 0$; thus a vanishing second-order work is signalled whenever the volumetric strain reaches a peak, i.e. $d\varepsilon_v = 0$. This is indeed verified in the numerical simulations presented in Figure 2a. The locus of points for which W_2 first vanishes defines a so-called instability surface evocative of Lade's instability line which arbitrarily connects the peaks of effective stress paths of loose sand responses under undrained conditions (Lade 1992). Here, in contrast with Lade's instability line, the treatment of instability carries both a mathematical and a physical meaning. Figure 2a reveals that the test can proceed past the bifurcation point due to the nature of the loading program, that is, stress-controlled. The test eventually aborts when the effective stress path reaches the plastic limit surface giving way to a different operating failure mode than the one (diffuse failure) at the bifurcation point. Controllability is only lost when stresses reach the failure line, depicted when $\det\mathbf{D} = 0$. That explains why even though the second-order work became negative much earlier the numerical simulation could be carried out past the instability line.

Next we show that if a similar test is carried out in mixed loading mode by imposing $dq = 0$ and $d\varepsilon_v < 0$, which emulates fluid injection into the specimen, the very same bifurcation locus is obtained. As seen in Figure 2b, the solution breaks down prematurely when $\det\mathbf{M} = 0$, which marks the loss of controllability, i.e.:

$$\begin{aligned}
 W_2 = dpd\varepsilon_v + dqd\gamma &= \begin{Bmatrix} d\gamma \\ dp \end{Bmatrix}^T \begin{bmatrix} M_{11} & M_{12} \\ M_{21} & M_{22} \end{bmatrix} \begin{Bmatrix} d\gamma \\ dp \end{Bmatrix} \\
 \text{with } \begin{Bmatrix} dq \\ d\varepsilon_v \end{Bmatrix} &= \begin{bmatrix} M_{11} & M_{12} \\ M_{21} & M_{22} \end{bmatrix} \begin{Bmatrix} d\gamma \\ dp \end{Bmatrix} \quad [6] \\
 \text{and } \begin{bmatrix} M_{11} & M_{12} \\ M_{21} & M_{22} \end{bmatrix} &= \frac{1}{D_{22}} \begin{bmatrix} \det\mathbf{D} & D_{12} \\ -D_{21} & 1 \end{bmatrix}
 \end{aligned}$$

where we have expressed the controlling parameters ($d\gamma$, dp) in terms of the response variables (dq , $d\varepsilon_v$) and de-

fining the matrix \mathbf{M} that relates ($d\gamma$, dp) to (dq , $d\varepsilon_v$). The matrix \mathbf{M} is a rearrangement of rows and columns of the constitutive matrix \mathbf{D} as shown above.

These examples reveal that the concepts of Hill's stability and Nova's controllability are indeed related. It is worth mentioning that Nicot & Darve (2009) have recently attempted to unify the framework for failure in geomaterials through the notion of sustainability, which covers Hill's and Nova's approaches. For example, Nicot & Darve (2009) demonstrated that when controllability is lost, the second-order work response is directly linked to the burst of kinetic energy as a small perturbation is applied. This concept is, however, out of the scope of this paper as it deserves a much in-depth consideration.

4.2 Boundary value problem level

In section 4.1, the homogeneous case in form of element tests was explored. Numerical findings were limited to prove the concept that instability could be embraced within the second-order work framework and the notion of controllability. Here, a more complete numerical analysis using a 3D representation of the soil specimen, including the interaction of a fluid phase and material heterogeneity, is pursued in order to model the actual constant shear lab experiments. As such, failure can be studied in an initial boundary value setting as various deformation modes emerge during loading history. The boundary value problem was modelled using the commercial finite element (FE) code Abaqus (2006).

The FE problem represents a cylindrical sand specimen 22 cm tall and 10 cm diameter as illustrated in Figure 3. Except for the nodes located on the bottom surface which are restricted to motion along z-component (vertical), displacements can take place in any direction elsewhere. The node located on the bottom surface and at the axis of geometrical symmetry was also restricted to displacements along components x and y and spin around the axis of symmetry in order to prevent rigid body and spin motions. A total of 5220 three-dimensional C3D8P elements with eight nodes and full integration were used in these simulations.

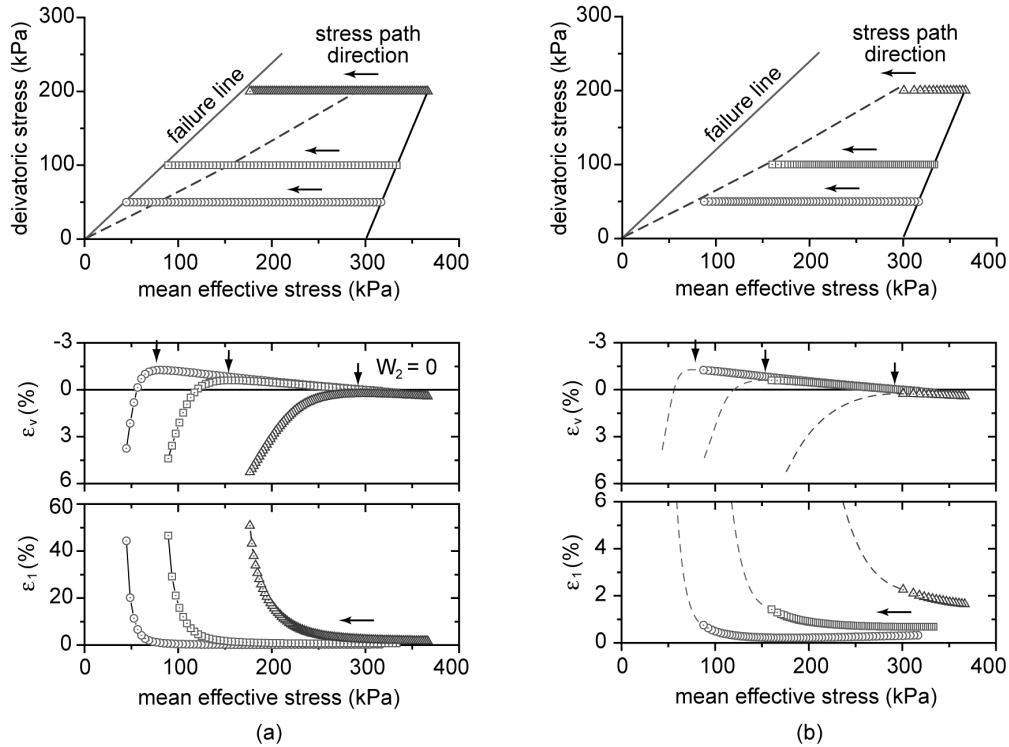


Figure 2. (a) Stress-controlled drained constant shear test (b) Mixed-controlled drained constant shear test. Dashed lines in (b) correspond to the stress-strain response obtained from the stress-controlled simulations.

The WG-model was implemented in Abaqus through the user material subroutine facility called UMAT. To ensure robustness in the plasticity calculations, an implicit stress return and consistent tangent operator algorithm together with spectral decomposition of the stress tensor were developed for the WG-model and implemented in UMAT (see Pinheiro & Wan 2010).

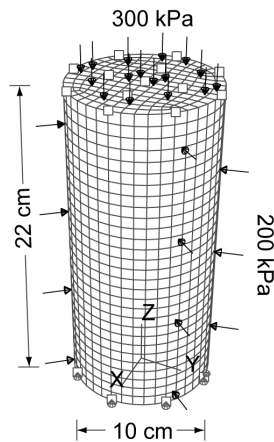


Figure 3. Initial mesh and boundary condition settings prior to pursuing the q-constant loading path

An initial imperfection was introduced in the specimen through material perturbation in the form of a ran

dom but not spatially correlated distribution of the initial void ratio field. A Gaussian (normal) distribution was chosen to describe the initial distribution of this field, as computer simulated 3D images of regular packing, irregular (non-spherical particles) packing and random uniform spherical packing seem to roughly suggest (Al-Raousha & Alshibli 2006). Other authors have used different stochastic distributions of void ratio, such as the truncated exponential distribution (Tejchman 2006, Andrade et al. 2008). The void ratio was spanned about a mean value of 0.70 with a standard deviation of 0.025, which corresponds to a hypothetical medium sand case as shown in Figure 4. The minimum and maximum values of void ratio reached were 0.62 and 0.79, respectively. These values are not based in any real soil sample; they were artificially introduced so as to set an initial perturbation on the homogeneous configuration of the boundary value problem.

Figure 5 shows snapshots of the second-order work distribution in the middle transversal section of the specimen at various times corresponding to the constant shear portion of the loading path. It is noted that darker zones refer to regions where the second-order work criterion has been violated ($W_2 \leq 0$). Given the initial void ratio fluctuation in space, every material point follows a different q-constant loading path, and hence the second order-work is violated heterogeneously throughout the specimen. At $t = 80$ s, the second-order work is pervasively violated throughout the specimen, corresponding to diffuse failure. Although all stress states are far from the plastic limit surface (mobilized friction angle is

around 24° as opposed to 32° at plastic limit), the sample is unstable according to Hill's stability criterion. Figure 5d ($t = 97s$) shows the evolution of second-order work past the bifurcation point as the specimen further deforms with the loading path approaching the plastic limit surface.

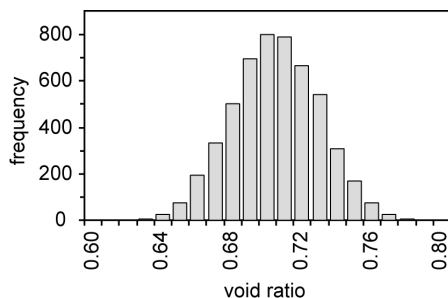


Figure 4. Histogram of void ratio frequencies for the randomly generated Gaussian distribution

There are three important observations: (a) A relatively rapid increase in deformations describing the transition from $t = 80s$ to $97s$ takes place as the plastic limit is approached ($t = 97s$ refers to the last converged step out of 100 steps or 100s). (b) Some zones of the specimen where W_2 was clearly negative now revert to positive values and hence regain stability. It is plausible to attribute this phenomenon to the emergence of a lightly localized failure pattern in the core of the specimen. In other words, shear bands do not clearly form but can still be delineated by regions where the second-order work remain negative as shown in Figure 5d. It is noted that within a localized zone, the second-order work is also negative as theoretical analyses based on the sign of the hardening modulus reveal. (c) The notion of controllability explains why the specimen did not collapse when its stresses entered the bifurcation region. In agreement with the element level simulations presented before, here the local constitutive tensor did not become singular at any finite element, which allowed us to maintain control over the test except when failure locus was eventually reached.

At element level, we showed a series of constant shear simulations where the specimen was forced to dilate monotonically. Those tests revealed that the control variables, q and ϵ_v , could no longer be controlled as soon as the bifurcation point identified by the zero-valued second-order work in pure drained q -constant tests was achieved. This interesting finding is also verified in the boundary value simulations presented in this paper. Here though, ϵ_v cannot be controlled directly. Instead, a small amount of fluid flux ($5E-4 \text{ m}^3/s$) is injected into top and bottom of the specimen so as to mimic a dilative path. Lateral boundaries are kept sealed to any in/out flux. At the same time, stresses on all boundaries are kept unaltered throughout the test so that deviatoric stress does not change. As fluid goes in the sample, pore pressure builds up and the effective stresses reduce at all ele-

ments. The forced dilatant path proceeds till the specimen cannot absorb fluid anymore. At this moment, finite element solution breaks down which corresponds to the specimen total collapse. As anticipated, this moment coincides with that where stresses enter the bifurcation zone.

Figure 6 compares the results from both CSD and constant shear test with force dilation to 15 nodes located along the transversal section of the specimen. The small circles on this figure indicate where Hill's stability criterion is first violated. What we tried to explain in words becomes much more apparent in the p - q plots of this figure. Figure 6 also brings an important conclusion about the evolution of void ratio. It shows that the sand specimen under force dilative path collapses at mean effective stress of around 130 kPa, which also roughly corresponds to the stress level where the specimen subjected to pure q -constant test shifts from a dilative to a contractive deformation mode.

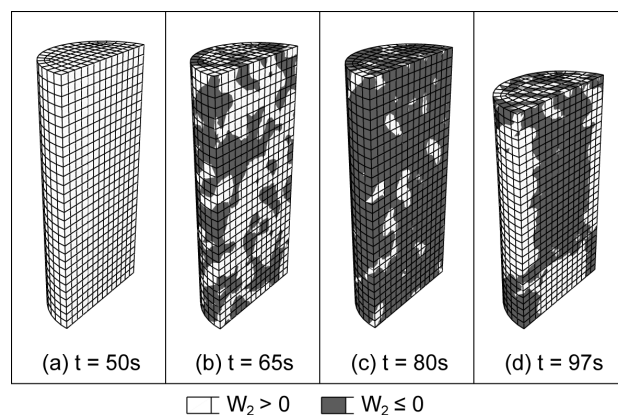


Figure 5. Evolution of second-order work in one-half meridional section of the specimen at various times during the q -constant loading path (x1 magnification)

5 CONCLUSIONS

This paper goes over recent theoretical, experimental and numerical studies of material instability in geomaterials. The condition of a plastic limit as defined by a Mohr-Coulomb criterion has virtually dominated the mathematical and computational analysis of failure. However, it is now fully recognized by experimental evidence and mathematical developments that there exist cases of failure where material instability can be manifested without any apparent discontinuity in kinematic field and the corresponding localized deformation. It is important to consider this so-called diffuse type of failure since it presents a lower bound to the plastic limit condition. We show that notions of loss of second-order work positiveness and controllability during a loading program are related. We also reveal that for the second-order work to vanish, one of the pre-requisites is to have a non-symmetric tangent constitutive tensor for describing the behaviour of the geomaterial. As such, we bring in an

elastoplastic model with a non-associated plastic flow rule as well as stress and void ratio dependencies that provide mathematical sources of material instability. This model successfully captures diffuse instabilities and subtleties in the effect of loading programs on the loss of controllability of a test. The constant shear lab experimental test is used as a prototype example to illustrate and validate the theoretical developments discussed in the first part of the paper.

ACKNOWLEDGEMENTS

The authors would like to acknowledge the financial support provided by the Natural Science and Engineering Research Council (NSERC).

REFERENCES

- Abaqus, 2006. *Abaqus/CAE: User's Manual*. Version 6.6, ABAQUS Inc, USA.
- Al-Raousha, R. and Alshibli, K.A. 2006. Distribution of local void ratio in porous media systems from 3D X-ray microtomography images. *Physica A*, 361: 441-456.
- Andrade, J.E., Baker, J.W. and Ellison, K.C. Random porosity fields and their influence on the stability of granular media. *Intl J. Num. Anal. Meth. Geomechanics*, 32: 1147-1172.
- Brand, E.W. 1981. Some thoughts on rain-induced slope failures. In *Proc. 10th Intl Conf. Soil Mech. Fnd Eng.*, Stockholm, Balkema, The Netherlands, 1: 373-376.
- Chu, J., Leroueil, S. and Leong, W.K. 2003. Unstable behaviour of sand and its implication for slope instability. *Can. Geotechnical J.*, 40: 873-885.
- Darve, F. 1994. Stability and uniqueness in geomaterials constitutive modeling. In *Localisation and Bifurcation Theory for Soils and Rocks*, Chambon et al. (eds), Balkema, 73-88.
- Darve, F., Sibille, L., Daouadji, A. and Nicot, F. 2007. Bifurcations in granular media: macro- and micro-mechanics approaches. *Comptes Rendus Mécanique*, 335: 496-515.
- Desrues, J. and Viggiani, G. 2004. Strain localization in sand: an overview of the experimental results obtained in Grenoble using stereophotogrammetry. *Intl J. Num. Anal. Meth. Geomechanics*, 28(4): 279-321.
- Hill, R. 1958. A general theory of uniqueness and stability in elastic-plastic solids. *J. Mech. Phys. Solids*, 6: 236-249.
- Imposimato, S. and Nova, R. 2001. On the value of the second-order work in homogeneous tests on loose sand specimens. In *Bifurcation and Localisation Theory in Geomechanics*, Muhlhaus et al. (eds), Swets & Zeitlinger: 209-216.
- Lade, P.V. 1992. Static instability and liquefaction of loose fine sandy slopes. *J. Geotech. Eng. ASCE*, 118(1): 51-71.
- Lade, P.V. 2002. Instability, shear banding, and failure in granular materials. *Intl. J. Solids Structures*, 39: 3337-3357.
- Nicot, F. and Darve, F. 2009. A unified framework for failure in geomaterials? In *Proc. 1st Intl Symp. Comp. Geomechanics (ComGeo I)*, G.N.. Pande and S. Pietruszczak (eds) Juan-les-Pins, France.

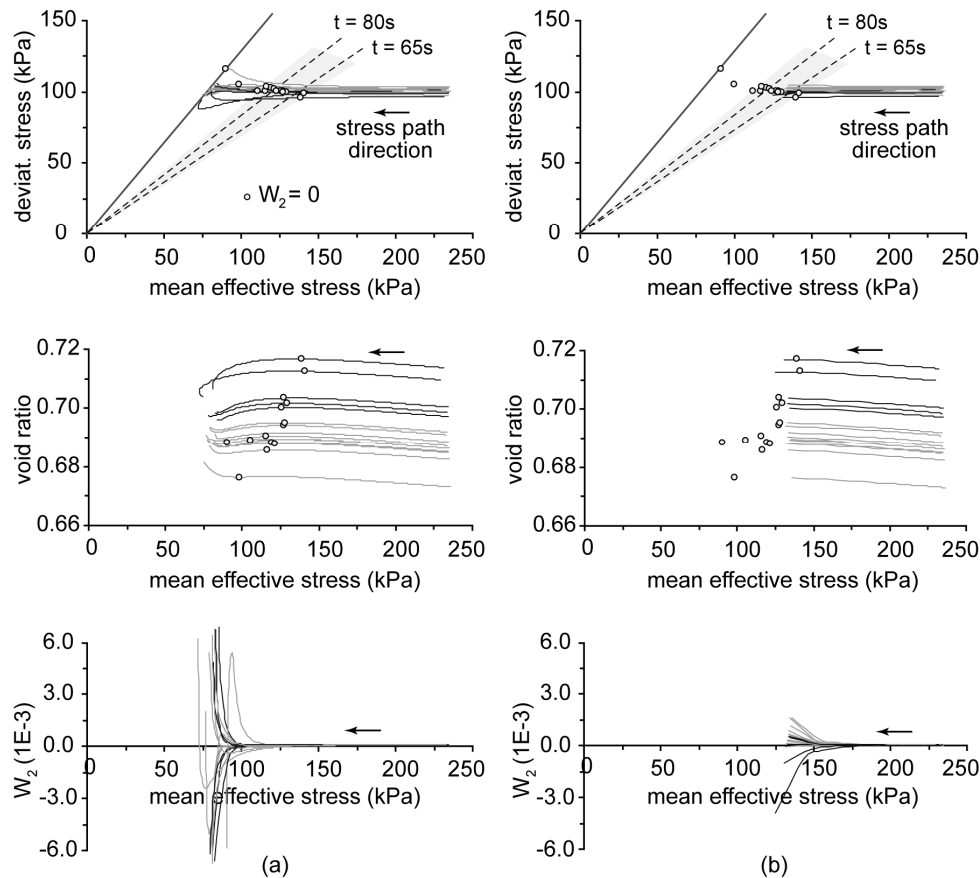


Figure 6. Constant shear test results for (a) controlled increase of pore pressure and (b) controlled volumetric increase through fluid injection

- Nova, R. 1994. Controllability of the incremental response of soil specimens subjected to arbitrary loading programs. *J. Mech. Behavior of Materials*, 5(2): 193-201.
- Nova, R. 2003. The failure concept in soil mechanics revisited. In *Bifurcations and Instabilities in Geomechanics*, J.F. Labuz and A. Drescher (eds). Balkema: 3-16.
- Pinheiro, M. and Wan, R.G. 2010. Finite element analysis of diffuse instability using an implicitly integrated pressure-density dependent elastoplastic model. *Finite Elements in Analysis and Design (21st Annual Robert J. Melosh Competition)*, 46(6): 487-495.
- Rowe, P.W. 1962. The stress-dilatancy relation for static equilibrium of an assembly of particles in contact. *Proc. Royal Society of London. Series A, Mathematical and Physical Sciences*, 269(1339): 500-527.
- Sasitharan, S., Robertson, P.K., Segoo, D.C. and Morgenstern, N.R. 1993. Collapse behavior of sand. *Can. Geot. J.*, 30: 569-577.
- Schofield, A.N. and Wroth, C.P. 1968. *Critical State Soil Mechanics*. McGraw-Hill, London.
- Tejchman, J. 2006. Effect of fluctuation of current void ratio on the shear zone formation in granular bodies within micro-polar hypoplasticity. *Computers and Geotechnics*, 33: 29-46.
- Wan, R.G. and Guo, P.J. 1998. A simple constitutive model for granular soils: modified stress-dilatancy approach. *Computers and Geotechnics*, 22(2): 109-133.
- Wan, R.G. and Guo, P.J. 2001a. Effect of microstructure on undrained behaviour of sands. *Can. Geot. J.*, 38: 16-28.
- Wan, R.G. and Guo, P.J. 2001b. Drained cyclic behavior of sand with fabric dependence. *J. Eng. Mech.*, 127(11): 1106-1116.
- Wan, R.G. and Guo, P.J. 2004. Stress dilatancy and fabric dependencies on sand behaviour. *J. Eng. Mech.*, 130(6): 635-645.
- Wan, R.G., Guo, P.J., Pinheiro, M. and Li, Q. 2008. Rupture par un Modèle Micromécanique Élastoplastique. In *Micromécanique de la Rupture dans les Milieux Granulaires, Traité MIM (Mécanique et Ingénierie des Matériaux)*, Hermes Science, F. Nicot and R.G. Wan (eds), Chapter 4; 141-175.

Wan, R.G., Pinheiro M. and Li Q. (2009) Granular material response with respect to loading direction and material instability. *Euro. J. Environ. and Civil Eng.* (EJECE), 13(2): 219-233.